Expression vector construct	Nucleotide residues	Amino acids	GenBank accession number	Generated by
GST-rPABP in pGEX-6P-3/371-636	1310-2107	371-636	AJ298278	PCR
rPABP in pFlag-tag 2B	203-2107	2-636	AJ298278	PCR
P1: EGFP-rPABP/2-636	203-2107	2-636	AJ298278	subcloning
P2: EGFP-rPABP/2-181	203-742	2-181	AJ298278	PCR
P3: EGFP-rPABP/82-276	443-1027	82-276	AJ298278	PCR
P4: EGFP-rPABP/179-370	734-1309	179-370	AJ298278	PCR
P5: EGFP-rPABP/371-636	1310-2107	371-636	AJ298278	PCR
rPABP in pGBKT7	203-2107	2-636	AJ298278	PCR
hMKRN1-short in pGEX-6P-2	7-1450	1-329	AM236048	subcloning
rMKRN1-short in pcDNA6/myc-His	4-990	1-329	BC079407	PCR
hMKRN1-short in pcDNA6/myc-His	7-993	1-329	AM236048	subcloning
T7-hMKRN1-short in pcDNA3	7-1450	1-329	AM236048	PCR
T7-hMKRN1-long in pcDNA3	159-1604	1-482	NM013446	PCR
M1: EGFP-hMKRN1-short	7-993	1-329	AM236048	PCR
M2: EGFP-hMKRN1-short/1-235	7-711	1-235	AM236048	PCR
M3: EGFP-hMKRN1-short/236-329	712-993	236-329	AM236048	PCR
M4: EGFP-hMKRN1-short/1-160	7-486	1-160	AM236048	PCR
M5: EGFP-hMKRN1-short/81-213	247-645	81-213	AM236048	PCR
M6: EGFP-hMKRN1-short/1-193+214-329	7-585+646-993	1-193+214-329	AM236048	PCR
M7: EGFP-hMKRN1-short/1-160+177-329	7-486+535-993	1-160+177-329	AM236048	PCR
M8: EGFP-hMKRN1-short/1-176+194-329	7-534+586-993	1-176+194-329	AM236048	PCR
M9: EGFP-hMKRN1-short/1-89+109-329	7-273+331-993	1-89+109-329	AM236048	PCR
M10: EGFP-hMKRN1-short/1-108+161-329	7-330+487-993	1-108+161-329	AM236048	PCR
M11: EGFP-hMKRN1-short/1-89+109-213+233-329	7-273+331-645+703-993	1-89+109-213+233-329	AM236048	PCR
M12: EGFP-hMKRN1-short/1-108+129-193+214-329	7-330+391-585+646-993	1-108+129-193+214-329	AM236048	PCR
pN22-Flag3-hMKRN1-short	7-993	1-329	AM236048	subcloning
pN22-Flag3-hMKRN1-short/1-160+177-329	7-486+535-993	1-160+177-329	AM236048	subcloning
pN22-Flag3-hMKRN1-short/1-176+194-329	1-176+194-329	1-176+194-329	AM236048	subcloning
pEGFP-PAM2$_{MKRN}$	487-585	161-193	AM236048	subcloning
hMKRN1-short in pBlueScript	7-486	n. a.	AM236048	PCR
pN22-Flag3-rShank3-1-290	10-879	1-290	AJ133120	PCR
pN22-Flag3-PAM2$_{MKRN}$-rShank3-1-290	Shank3: 10-879 MKRN:487-585	Shank3: 1-290 MKRN1:161-193	AJ133120 AM236048	subcloning
pN22-hDDX6	43-1458	1-486	AB527511	PCR
EGFP-IMP1	255-1988	1-577	BC161831	PCR
EGFP-IMP1-RRM 1+2	255-544	1-181	BC161831	PCR

Supplement TABLE 1. **Summary of expression vector constructs obtained by either PCR amplification or subcloning procedures.**
DDX, DEAD-box family of putative RNA helicases; EGFP, enhanced green fluorescent protein; GST, glutathione-S-transferase; h, human; IMP1, insulin-like growth factor 2 (IGF-2) mRNA-binding protein 1; MKRN, Makorin; PABP, poly(A)-binding protein; PAM, PCI/PINT associated module; PCR, polymerase chain reaction; r, rat; Shank3, SH3 and multiple ankyrin repeat domains protein 3.

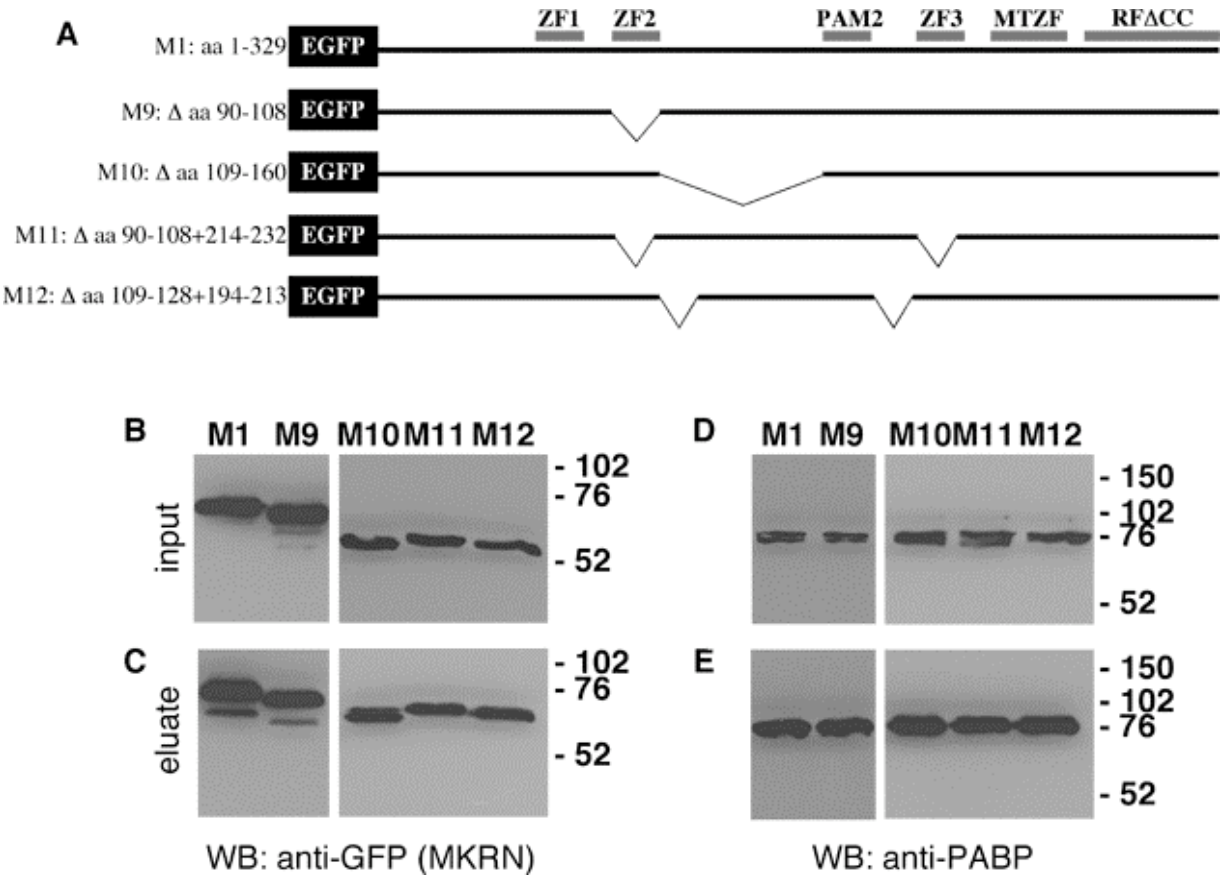

Supplement FIGURE 1. **Deletion of various parts of the central region of MKRN1-short does not impair its ability to interact with PABP.** A, Schematic representation of recombinant EGFP-MKRN1-short fusion proteins (encoded by M1 and M9-M12) that were transiently expressed in HEK-293 cells together with Flag-PABP. B-E, Protein extracts were subjected to immunoprecipitation with anti-Flag agarose followed by SDS-PAGE and Western blot (WB) analyses using anti-GFP antibodies for detection of EGFP-MKRN1 and its deletion mutants (B, C) or anti-PABP antibodies (D, E). The inputs are shown in B and D; the immunoprecipitates eluted from the beads are shown in C and E. The positions of molecular size marker proteins (in kDa) are indicated on the right. Experimental details are described in "Experimental Procedures". E, EGFP, enhanced green fluorescent protein; MKRN, Makorin; MTZF, Makorin-type zinc-finger; PABP, poly(A)-binding protein; PAM, PCI/PINT associated module; RFΔCC, truncated RING-finger domain; ZF, zinc-finger.

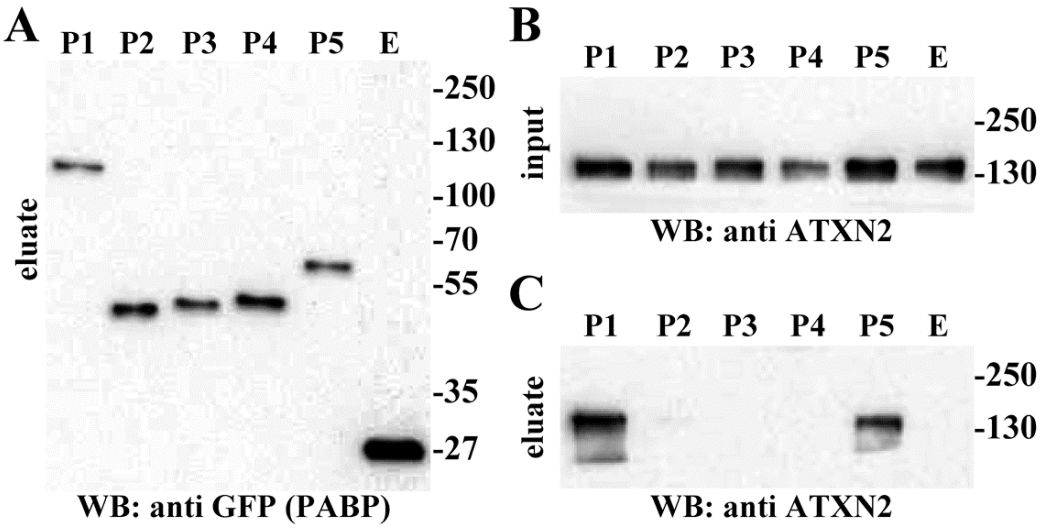

Supplement FIGURE 2. **Ataxin-2 (ATXN2) interacts only with the MLLE domain of PABP.** For this Western blot analysis, the extracts of HEK-293 cells transfected with EGFP-PABP deletion mutants (P1-P5) or an empty EGFP vector (E) along with T7-MKRN1-short (shown in Fig. 4) were used to confirm that ATXN2 exclusively interacts with the PABP C-terminal MLLE domain. Interaction with the N-terminal RNA recognition motifs is not observed. PABP constructs P1-P5 are schematically shown in Fig. 4 A. As outlined in the legend to Fig. 4, immunoprecipitations were done with GFP-Trap®_A. Proteins were resolved by SDS-PAGE, blotted onto nitrocellulose and probed with A, rabbit anti-GFP antibodies to detect recombinant EGFP-PABP, EGFP and B, C, mouse anti-ATXN2 antibodies for detection of endogenous ATXN2. HRP-conjugated secondary antibodies were used, and bound antibodies were revealed by chemiluminescent assays. Eluate, eluted immunoprecipitates; input, protein extracts prior to immunoprecipitation. The positions of molecular size marker proteins (in kDa) are indicated on the right. EGFP, enhanced green fluorescent protein.

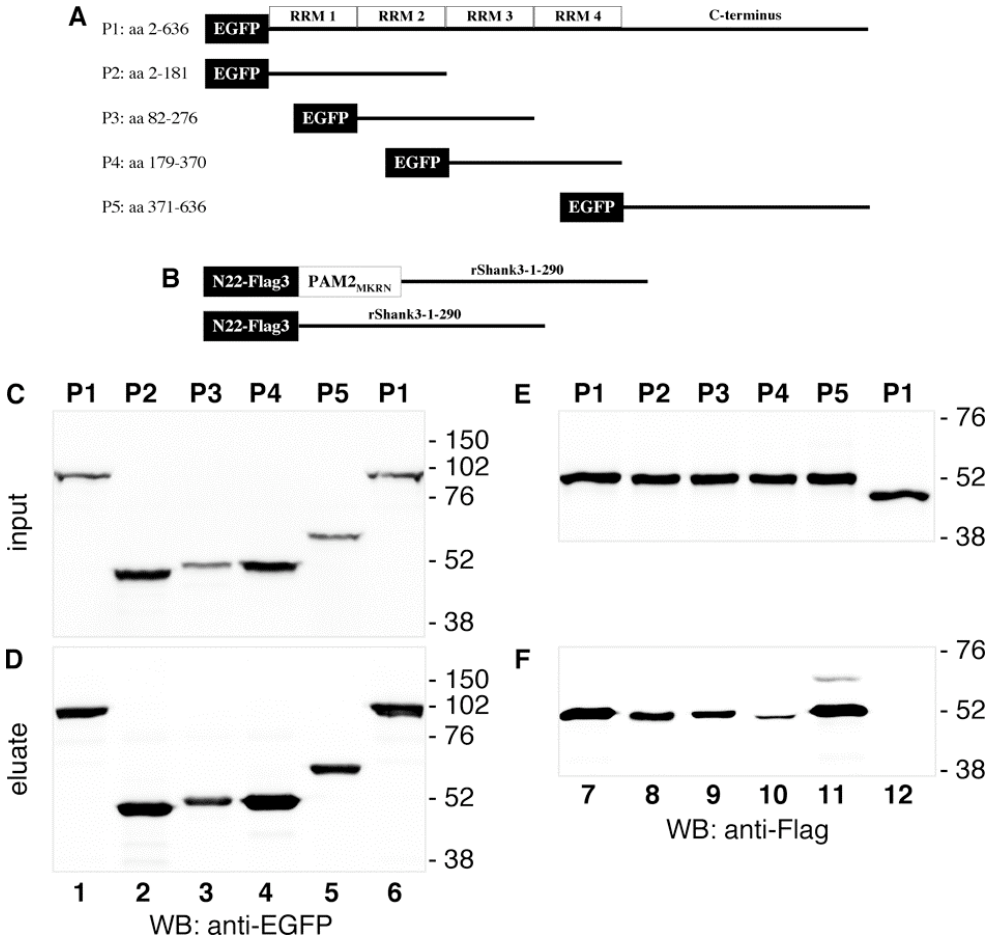

Supplement FIGURE 3: **The MKRN1-short PAM2-like domain alone mediates interaction with both the RRMs and the C-terminus of PABP.** A, Schematic representation of recombinant EGFP-PABP fusion proteins (encoded by P1-P5, see Supplement Table 1) that were transiently expressed in HEK-293 cells together with recombinant N22-Flag3-PAM2$_{MKRN}$-rShank3-1-290 or the control vector N22-Flag3-rShank3-1-290, as schematically shown in (B). The fusion protein N22-Flag3-rShank3-1-290 encodes the N-terminal part of the postsynaptic scaffold protein Shank3 that is not known to play any role in RNA metabolism (Naisbitt et al., 1999). C-F, Protein extracts were subjected to immunoprecipitation with GFP-Trap®_A beads followed by SDS-PAGE and Western blot (WB) analyses using anti-GFP antibodies for detection of recombinant EGFP-PABP proteins (lanes 1-6) and anti-Flag antibodies for detection of N22-Flag3-PAM2$_{MKRN}$-rShank3-1-290 (lanes 7-11) or the control protein N22-Flag3-rShank3-1-290 (lane 12). The inputs are shown in C and E, the immunoprecipitates eluted from the beads are shown in D and F. The positions of molecular size marker proteins (in kDa) are indicated on the right. The N22-Flag3-vectors and experimental details are described in "Experimental Procedures" and in Supplement Table 1.
aa, amino acid; EGFP, enhanced green fluorescent protein; PABP, poly(A)-binding protein; RRM, RNA recognition motif; Shank, SH3 and multiple ankyrin repeat domains protein.

Reference:
Naisbitt, S., Kim, E., Tu, J. C., Xiao, B., Sala, C., Valtschanoff, J., Weinberg, R. J., Worley, P. F., and Sheng, M. (1999) *Neuron* **23**(3), 569-582

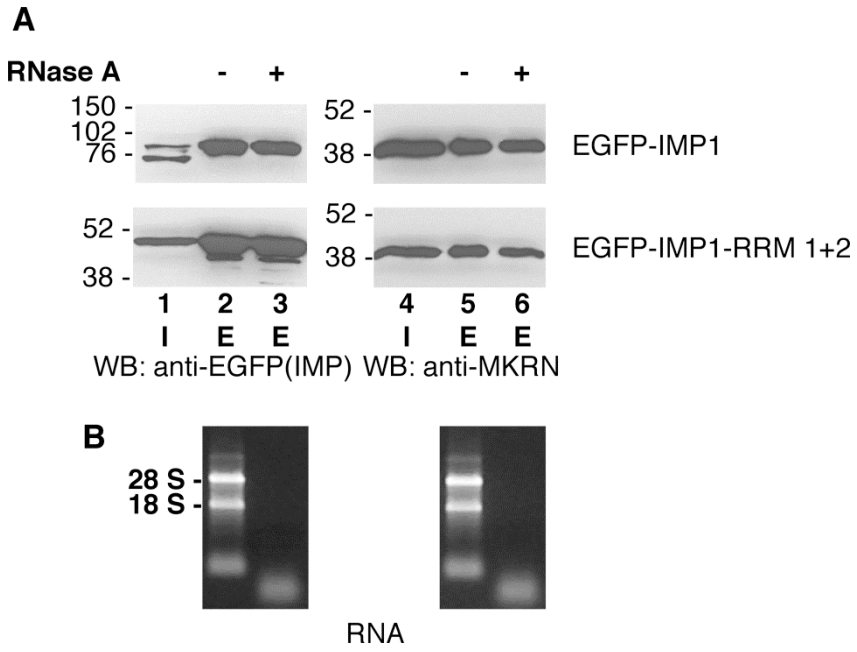

Supplement FIGURE 4. **MKRN1-short interacts with the IMP1-RRM domains in an RNA-independent manner.** T7-MKRN1-short was co-expressed in HEK-293 cells along with EGFP-tagged full-size IMP1 (EGFP-IMP1) or a construct encoding the IMP1 RRM domains 1+2 (EGFP-IMP1-RRM 1+2). A, Protein lysates were subjected to immunoprecipitation with GFP-Trap®_A beads in the presence (+) or absence (-) of RNase A followed by SDS-PAGE. Subsequently, Western blot (WB) analyses were performed using anti-GFP antibodies for detection of EGFP-IMP1 proteins (lanes 1-3), and anti-MKRN antibodies for detection of recombinant T7-MKRN1-short (lanes 4-6). I, input; E, protein eluted from GFP-Trap® beads. The positions of molecular size marker proteins (in kDa) are indicated on the left. B, RNAs extracted from non-digested lysates (lanes 2 and 5) and from lysates digested with RNase A (lanes 3 and 6) were resolved by agarose gel electrophoresis followed by ethidium bromide staining. The positions of the 18 S- and 28 S ribosomal RNAs are indicated on the left. The vectors encoding EGFP-IMP1 fusion proteins and experimental details are described in Supplement Table 1 and "Experimental Procedures", respectively. EGFP, enhanced green fluorescent protein; IMP1, insulin-like growth factor 2 mRNA-binding protein 1; MKRN, Makorin; RRM, RNA recognition motif.

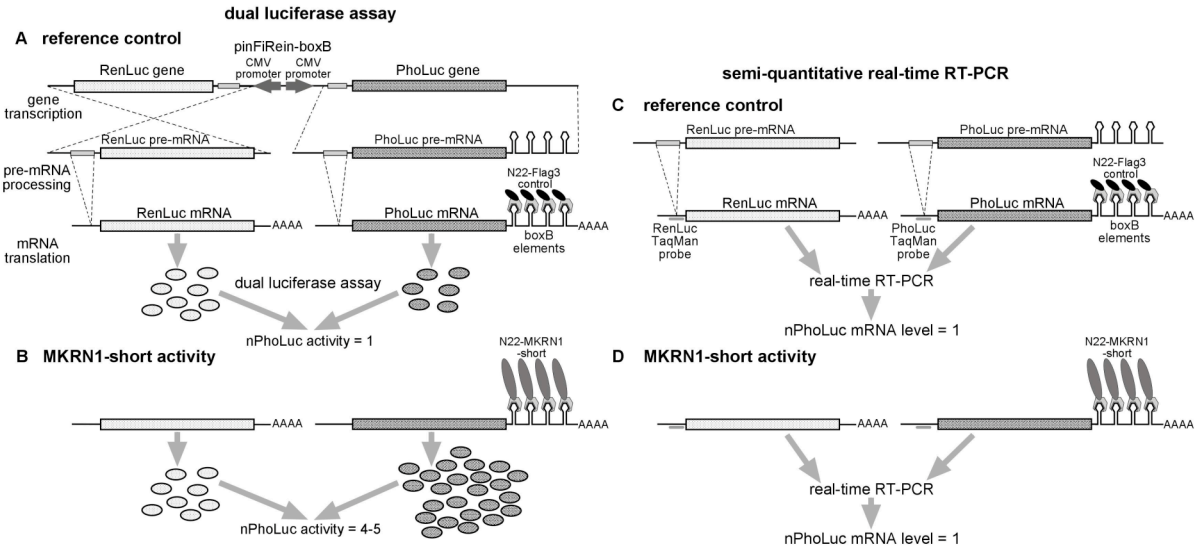

Supplement FIGURE 5: **Schematic representation of the N22-tethering assay**. A, Eukaryotic expression vector pinFiRein-boxB16B (upper line) contains two separate genes, both of which are driven by independent CMV promoters (dark grey horizontal arrows) and contain an intron (light grey small box) upstream of the region encoding *Renilla-* (RenLuc) or *Photinus* luciferase (PhoLuc; lightly and heavily stippled box, respectively). Primary neurons were co-transfected with pinFiRein-boxB16B and each with one of several vectors encoding distinct N22 fusion proteins, which are tethered to boxB stem-loop motifs in the 3'-UTR of PhoLuc mRNAs. Cells expressing fusion proteins consisting of N22 (light grey hexagon) and three tandem Flag epitopes (black oval) served as a reference control, in which the activity of PhoLuc (heavily stippled oval) normalized against the activity of RenLuc (lightly stippled oval) was arbitrarily set to 1. B, When tethered to PhoLuc reporter transcripts N22-tagged MKRN1-short (dark grey oval) led to a 4-5-fold increase in normalized PhoLuc activity. C and D, Semi-quantitative real-time RT-PCR analysis was performed with TaqMan® probes (short horizontal grey lines) hybridizing to sequences in RenLuc- and PhoLuc transcripts, respectively, which are derived from two neighboring exons. Notably, normalized PhoLuc mRNA levels obtained from cells expressing either the N22-Flag3 reference control (C) or N22-tagged MKRN1-short (D) were found to be identical. For more details on the tethering assay, see text. nPhoLuc, normalized Photinus luciferase.

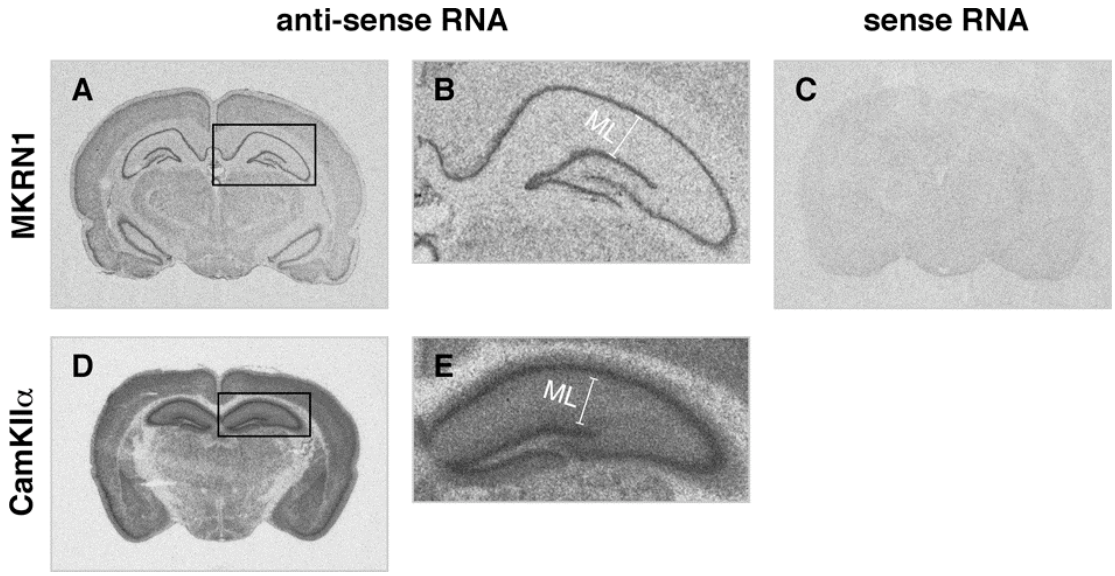

Supplement FIGURE 6: **MKRN1 mRNA is not localized to dendrites of hippocampal neurons.** A, An adult rat brain section was hybridized to an ^{35}S-labelled MKRN1 anti-sense riboprobe (transcribed from clone hMKRN1-short in pBlueScript, see supplement Table 1). B, Higher power magnification of the hippocampal formation encircled by the rectangle in (A) reveals that MKRN1 mRNA is confined to cell body layers. C, Control section hybridized to a sense RNA probe. For comparison, the distribution of the dendritically localized Ca^{2+}/calmodulin-dependent protein kinase α-subunit (CamKIIα) mRNA in a mouse brain section is shown in D. Note the intense labelling of dendrites in the molecular layer (ML). E, Higher power magnification of the hippocampal formation encircled by the rectangle in (D). Preparation of brain sections, generation of radiolabellled riboprobes, performance of *in situ* hybridizations and exposure to X-ray film was done as described (Macias *et al*. 2002). MKRN, Makorin.

Reference:

Macias, M., Fehr, S., Dwornik, A., Sulejczak, D., Wiater, M., Czarkowska-Bauch, J., Skupa, M., and Schachner, M. (2002) *Mol. Neurosci* **13**(18), 2527-2530

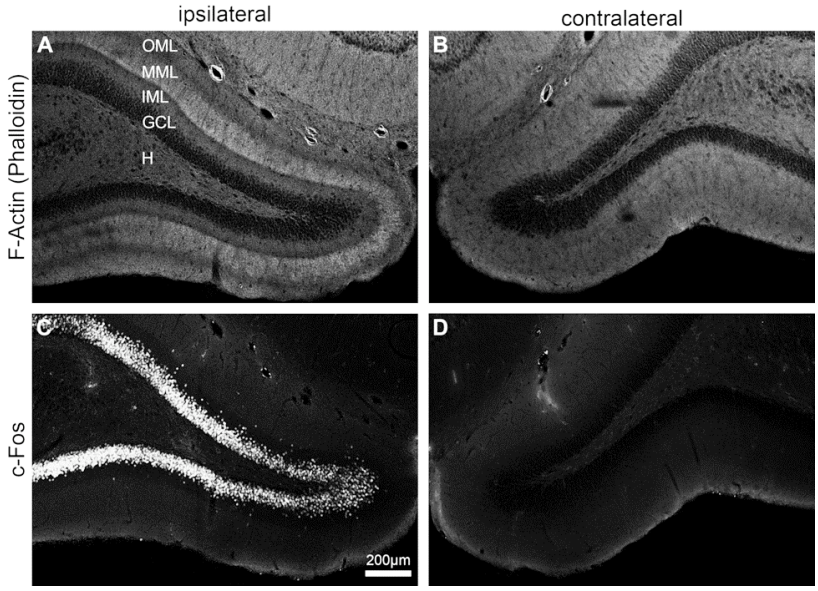

Supplement FIGURE 7. **Induction of long-term potentiation (LTP) leads to reorganization of microfilaments and induces robust *c-fos* gene expression.** High frequency stimulation (HFS) of the perforant path in adult urethane anaesthetized rats leads to an increase in F-Actin within the ipsilateral middle molecular layer (MML) of the dentate gyrus (DG), the site of maximal medial perforant path afferent innervation (A). In addition, the immediate early gene *c-fos*, a marker of synaptic activity, is expressed in more than 95% of cells in the ipsilateral granule cell layer (GCL, C). The DG contralateral to the stimulated side did not show increased labeling (B, D). HFS was applied for 2 h to maximally evoke population spikes and induce robust LTP as has been described (35). For F-Actin staining, coronal 50 µm hippocampal sections were incubated with Alexa Fluor® 488 Phalloidin (1:2000, MoBiTec) for 4h at 4°C. C-Fos immunostaining was performed with anti-c-Fos antibodies (rabbit, polyclonal, 1:1000, Santa Cruz, Ctl. Sc-52-G). H, hilus; IML, inner molecular layer; OML, outer molecular layer.

Reference

Schwarzacher, S.W., Vuksic, M., Haas, C. A., Burbach, G. J., Sloviter, R. S., and Deller, T. (2006) *Glia* **53**(7), 704-714